EVLA Memo 159
Interferometric observations with self noise - An example

R.J. Sault

May 2, 2012

Introduction

"Self noise" is the term used in radio observations where the power contributed by the astronomical source is a significant portion of the total received power. Self noise results in a degradation of system sensitivity compared to an observation of a near-blank field. This degradation can be substantial. This memo considers some cases where the correct accounting for self noise on sensitivity is important in understanding the VLA response. We give an example of the search for a Zeeman (Stokes V) signature in a maser observation.

Because self noise requires a strong source, its consequences are often less important than it might first seem. It may not be important if there is additional noise on top of a strong source. However self noise will be significant if the science is not concerned with the strong source, but with another weaker component. Examples of this include:

- a weak source in the same field as a strong confusing source;
- a strong source with weak polarized emission; or
- a strong continuum source with a weak spectral signature (note that continuum subtraction will not subtract out self noise).

Self noise basics

For single dish observations, accounting for self noise in the sensitivity calculation is relatively straightforward: the source power contributes to the system temperature used in the radiometer equation:

$$\sigma^2_{\text{single dish}} = \frac{1}{B\tau}(S_\text{a} + S_\text{s})^2,$$

where S_a is the antenna system equivalent flux density (SEFD) for a blank field and S_s is the source flux density, B is the observing bandwidth and τ is the total integration time. This is for a single polarization. Note that the noise from orthogonal polarization measurements (both antenna and source components) is independent. The SEFD for an antenna is

$$S_\text{a} = \frac{2kT_\text{sys}}{\epsilon A}$$

where k is Boltzman's constant, A is the collecting area, ϵ is an efficiency (the combination of antenna efficiency and the efficiency of the receiver and digital back-end) and $T_{\rm sys}$ is the system temperature. SEFD decreases with more collecting area and lower system temperature. For a strong source with appreciable spectral structure (e.g. a maser), the sensitivity will be a function of frequency. For very strong source and/or very large/sensitive antennas, i.e. $S_{\rm s} >> S_{\rm a}$, the system power can be dominated by the source emission. In this case, the overall sensitivity is not determined by the telescope but by the source. In this extreme case, the sensitivity is independent of the collecting area and receiver technology. It may be just as effective to use a small antenna with a simple receiver to a large, sensitive one.

For an interferometer array, there are some subtleties depending on whether or not the strong source emission is resolved or not. We will consider only the two extreme situations: either

- the strong source is completely resolved out on all baselines; or
- the strong source is completely unresolved.

Fuller details, including the intermediate cases, are considered by Kulkarni (AJ 1989), Vivekanand & Kulkarni (1991, ASP Conf Series vol. 19) and Anantharamaiah et al (1991, ASP Conf Series vol. 19). Also see Wrobel & Walker (1999, ASP Conf Series vol. 180) for a broader discussion of sensitivity.

For the case where the strong source is completely resolved out, the source contribution can be thought of as an additional component to the system temperature. In this case, the variance for a baseline and the array are

$$\begin{aligned}
\sigma^2_{\rm baseline} &= \frac{1}{2B\tau}\big(S_{\rm a}+S_{\rm s}\big)^2, \\
\sigma^2_{\rm array} &= \frac{1}{B\tau N(N-1)}\big(S_{\rm a}+S_{\rm s}\big)^2 \\
&\approx \frac{1}{B\tau}\big(\frac{S_{\rm a}+S_{\rm s}}{N}\big)^2.
\end{aligned}$$

Here N is the number of antennas, and we assume (for simplicity) that all antennas have the same SEFD and are combined with equal weight. The variance is the same for both the real and imaginary parts of the visibility. A classical example is an observation in the galactic center where there is very strong, large-scale synchrotron emission. For many interferometer arrays, this large scale structure will be completely resolved out but will contribute significantly to system power.

For the case where the strong source is unresolved, it is simplest if we consider the array to be phased up to be centered on the source. The variances on the real and imaginary parts will differ: the real part will be affected by the source whereas the imaginary part will not. In particular, the variance for a baseline and the array, for the real part are:

$$\begin{aligned}
\sigma^2_{\rm baseline,rp} &= \frac{1}{2B\tau}\big(S^2_{\rm a}+2S_{\rm a}S_{\rm s}+2S^2_{\rm s}\big), \\
\sigma^2_{\rm array,rp} &= \frac{1}{B\tau N(N-1)}\big(S^2_{\rm a}+2(N-1)S_{\rm a}S_{\rm s}+N(N-1)S^2_{\rm s}\big) \\
&\approx \frac{1}{B\tau}\big(\frac{S_{\rm a}}{N}+S_{\rm s}\big)^2.
\end{aligned}$$

Unlike the "resolved out" case, the self noise contribution does not average down with the number of baselines. As the source is unresolved, the self noise is the same on all baselines. An alternative way of understanding this is in terms of a phased array. In this case, the sensitivity should match the single dish case with the effective

SEFD of the phased array being $S_{\rm a}/N$[1]

The variance of the imaginary part is simpler: because we have assumed the data are phased up on the source, there is no contribution by the source to the variance of the imaginary part:

$$\begin{aligned}\sigma^2_{\rm baseline,ip} &= \frac{1}{2B\tau}S_{\rm a}^2,\\ \sigma^2_{\rm array,ip} &= \frac{1}{B\tau N(N-1)}S_{\rm a}^2\\ &\approx \frac{1}{B\tau}\left(\frac{S_{\rm a}}{N}\right)^2.\end{aligned}$$

Because the real and imaginary parts have different variances, the noise in an image formed from these data will vary with position. In images, the variance resulting from self noise component will be modulated by the square of the point-spread function around the strong source.

For emission that is resolved out, self noise will need to be accounted for when $S_{\rm s} \sim S_{\rm a}$. However for sources that are unresolved, self noise should be accounted for when $S_{\rm s} \sim S_{\rm a}/N$. For the VLA, where an antenna SEFD is typically about 300 Jy, self noise should be included when analyzing point sources stronger than about 11 Jy. As a comparison, for a hypothetical SKA-like array with 10,000 10 m antennas, each with SEFD of 2000 Jy, accounting for self noise will be important for sources stronger than 200 mJy. Typically there would be a handful of such sources in each field. But note again that the variance of the self-noise component is modulated by square of the point-spread function. So for an SKA-like array with very low imaging sidelobes, the self-noise component may not be important away from the source itself. Clearly the importance of self noise to an SKA-like array will depend on the details of the observing strategy and the science that is to be derived.

Self noise and self calibration

When a field has strong sources, self calibration will usually be performed on the data. In a field with a single strong source, the self noise from that source will be hidden to some degree by amplitude self calibration. If amplitude self calibration solutions are determined at the correlator dump rate, the amplitude gains will completely subsume the self noise self noise fluctuation. Similarly, for a spectral line observations where amplitude self calibration is performed over a range of channels, a part of the self-noise fluctuation will be subsumed into the amplitude gain solutions. When self calibrating a field with multiple strong sources, self noise could be mistaken as direction-dependent gains. Self noise will certainly limit the performance of amplitude self calibration for fields with many strong point sources. Classical amplitude self calibration will be inadequate for SKA-like arrays.

While amplitude self calibration may be an adequate tool for handling self noise from in field with a single very dominant point source, it would not be appropriate for more complex fields. For fields with a number of strong point sources, it would be more appropriate to use techniques that aim to remove self noise through sky position-dependent temporal low-pass filtering.

An example

This memo was triggered by the search for a Zeeman (Stokes V) signature in a strong galactic methanol maser where self noise was significant. Because self noise was not accounted for in the analysis, there was appreciable

[1]The phased array is not strictly correct analog. Because interferometer arrays do not include the autocorrelations, there is a factor in the variance of $N/(N-1)$ difference between an interferometer array and a phased array.

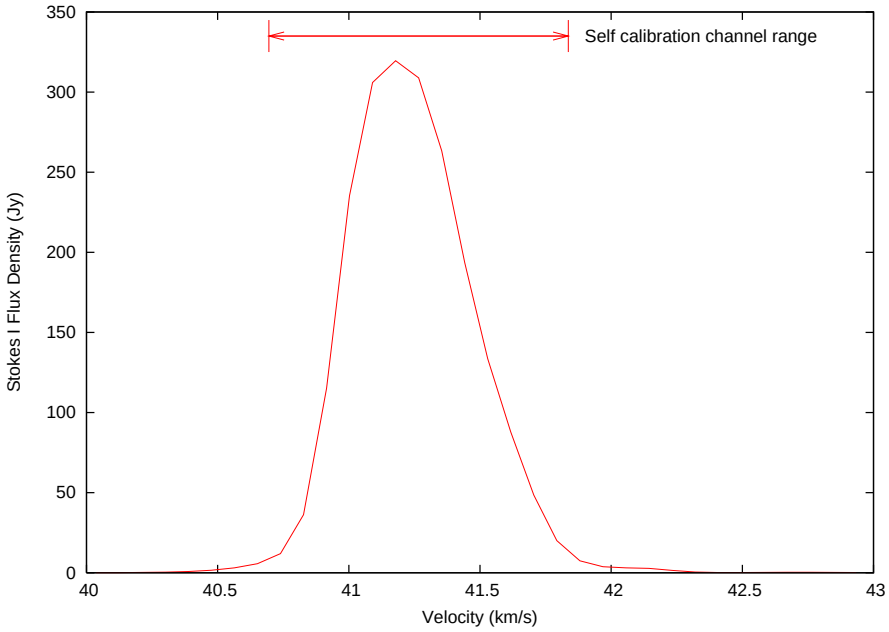

Figure 1: The maser line.

concern that the VLA was not functioning correctly during the observations. Here we briefly analyse these observations.

The 6.7 GHz methanol maser in question was g37.40+1. Figure 1 shows a Stokes-I spectrum of the source. Observations were taken on 25 March, 24 May, 3, 4 and 14 June, 24 and 25 September 2011, which gave a mixture of the B and A array configurations. Generally the maser was unresolved by both these arrays. For some baselines in A configuration, the maser was resolved: these baselines were discarded. The observations used correlator configurations without recirculation giving 256 or 128 channels with 0.98 or 1.95 kHz frequency resolution respectively. Data were averaged to 1.95 kHz resolution where needed. The maser width is about 30 kHz. Data were brought onto a single velocity grid by performing integral channel shifts to the visibility spectra. Because the line is broad, integral channel shifts, with its easily understood side effects, was seen as preferable to more sophisticated interpolation schemes (there was concern about possible interpolation artifacts).

The strength of the maser as well as the high dynamic range requirements of the experiment drove the calibration to be moderately unconventional. A phase slope was solved for across the maser emission. This phase slope was primarily a result of the maser not being placed at the phase center of the observation. Otherwise no bandpass calibration was performed. Bandpass calibration was believed to more likely introduce error rather than correct it. The lack of bandpass calibration places a stringent requirement on the similarity of the RR and LL bandpasses. The digital component of the bandpass will be identical for RR and LL. The RF component over such a small bandwidth should be essentially constant or a slope. Different quadratic components of the RR and LL bandpasses would be needed to eliminate a Zeeman Stokes V "S" signature. This is possibly the largest uncorrected systematic in the result.

No polarization calibration was done. By not performing any polarization calibration, there is a potential for Stokes Q and U signatures to leak into the Stokes V. Separate observations showed the Stokes Q and U signals

were less than a few Jansky. Leakage of Stokes quantities of this strength would not lead to significant false Stokes V in our results.

Antenna gains (amplitude and phase) for RR and LL were determined by self calibrating the sum of the 14 channels where the Stokes-I flux density was more than about 5% of the peak. The self-calibration solution interval was set to the correlator dump time. The amplitude self calibration was driven in a manner to give a peak flux density of 325 Jy. This was the peak flux density found from early calibration using a standard flux calibrator. Doing amplitude self calibration in this manner will subsume some of the channel self noise into the self-calibration gains. This will reduce the variance of the self noise by a factor of 13/14, which we have ignored.

This approach to determining the antenna gains means that the Stokes V signature, when averaged over the self-calibration channel range, will be forced to be 0. As Zeeman experiments are expected to give "S" curves, this calibration approach may distort the Zeeman signature (if the signature is not equally positive and negative), but it would not eliminate it. It is important that the range of channels used for self-calibration should fully cover the channels which could plausibly have Stokes V emission.

Figure 2 shows the Stokes V formed by summing all the visibility spectra. Both a real part and imaginary part are shown. As well as the spectrum, an envelope corresponding to $+1\sigma$ and -1σ has been drawn. The variance of the real and imaginary parts of the summed visibility spectrum go as

$$\begin{aligned} \sigma_{\rm rp}^2 &\propto \left(\frac{S_{\rm a}}{N} + S_{\rm s}\right)^2, \\ \sigma_{\rm ip}^2 &\propto \left(\frac{S_{\rm a}}{N}\right)^2. \end{aligned}$$

So for $N = 27$ antennas, each with nominal SEFD of $S_{\rm a} = 300$ Jy and a Stokes I strength peaking at $S_{\rm s} = 325$ Jy, we see the σ for the real part varies by a factor of 30 between the channel at the peak of the emission and the channels with no emission. Similarly the σ of the real part at the peak of the emission is 30 times greater than the σ of the imaginary part. Clearly understanding the self noise contribution is critical to understanding the noise properties of the spectrum. There is at best a few sigma Stokes-V detection. The rms Stokes V to peak Stokes I is about 10,000. The imaginary part is somewhat discrepant from the expectation, but not excessively so. This discrepancy was found to be predominantly from one days data.

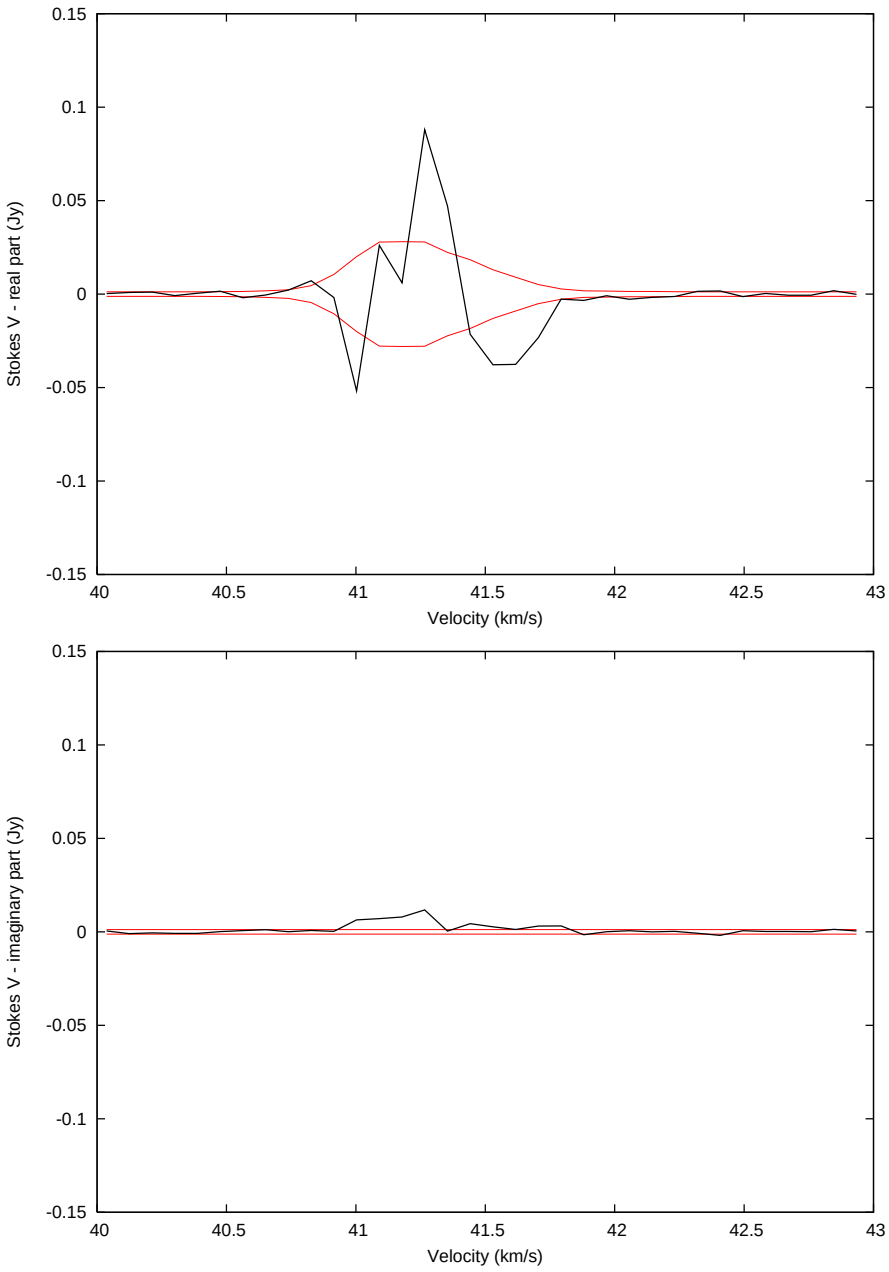

Figure 2: The real and imaginary part (top and bottom panels) of the summed Stokes V spectrum. Each plot also shows an envelope corresponding to $+1\sigma$ and -1σ.